

Microstructures and characteristics of deep trap levels in ZnO varistors doped with Y₂O₃

LIU Jun¹, HU Jun¹, HE JinLiang^{1†}, LIN YuanHua² & LONG WangCheng¹

¹ State Key Laboratory of Power Systems, Department of Electrical Engineering, Tsinghua University, Beijing 100084, China;

² State Key Laboratory of New Ceramics and Fine Processing, Department of Material Science and Engineering, Tsinghua University, Beijing 100084, China

In this paper discussions on ZnO based varistor ceramics doped with different ratios of Y₂O₃ are presented. Analysis on the phase and microstructures of the samples indicates that an additional phase is detected in the samples doped with Y₂O₃, and the average grain size of the specimens decreases from about 9.2 μm to 4.5 μm, with an increase in the addition of Y₂O₃ from 0 mol% to 3 mol%. The corresponding varistor's voltage gradient markedly increases from 462 V/mm to 2340 V/mm, while the nonlinear coefficient decreases from 22.3 to 11.5, respectively. Furthermore, the characteristics of deep trap levels in these ZnO samples are investigated by measuring their dielectric spectroscopies. The trap energy level and capture cross section evaluated by relaxation peak of the Cole-Cole plot vary slightly as the addition of Y₂O₃ increases. These traps may be ascribed to the intrinsic defects of ZnO lattice.

ZnO, varistors, Y₂O₃, electrical properties, deep trap levels

1 Introduction

ZnO varistors have been widely used in electrical power systems against overvoltage surges for their excellent characteristics of nonlinearity, stability and energy absorption capability^[1,2]. Nowadays, with the rapid growth of power consumptions, 1000 kV ultra-high voltage (UHV) AC transmission line has been put into operation, and a UHV power grid is being constructed, this leads to the requirement of UHV surge arresters based on high voltage gradient ZnO varistors^[3]. It has been generally believed that the double Schottky barrier formed at the grain boundary is the origin of the nonlinear characteristics of the ZnO varistor. Usually, the breakdown voltage of the ZnO varistor is about 3 V per grain boundary. However, the grain size of the traditional varistor is about several tens of micrometers, and as a result, its voltage gradient is limited far below the demands of UHV and GIS power systems. Generally, it was suggested to develop high voltage gradient ZnO varistors by inhibiting the grain growth^[4]. It has been reported re-

cently that some rare earth oxide was considered as a grain growth inhibitor^[5-7]. As a result, the electrical properties of ZnO based varistor ceramics were markedly influenced by the introduction of the rare earth oxides.

The inspection of dielectric spectroscopy in the complex plane could reveal the strong influence of deep trap energy characteristics upon the observed response of the varistor sample. This technique has been greatly introduced in the study of electroceramic materials. The complex plane representation is meaningful in discussions of electrical conduction mechanism and relaxation behavior. For instance, the response time, the low frequency capacitance, and the capability to withstand transient overvoltage surges of ZnO varistors largely depend on the capture and emission rate of electrons

Received June 8, 2009; accepted July 29, 2009

doi: 10.1007/s11431-009-0369-9

† Corresponding author (email: hejl@mail.tsinghua.edu.cn)

Supported by the National Natural Science Foundation of China (Grant Nos.50425721 and 50737001) and the 11th Five-year Natural S&T Supporting Plan of China (Grant No. 2006 BAA02A16)

obtained from the dielectric spectroscopy. Hence, it is necessary to investigate the characteristic of deep trap in ZnO varistors in order to understand and control their effect on the static and dynamic electrical response of the varistor. Alim presented a generic complex capacitance plot of a metal oxide varistor, which contained multiple relaxations and a resonance phenomenon in different frequency ranges^[8,9]. Three distinct relaxation times denoted as τ_2 , τ_3 and τ_4 in low and intermediate frequency range can be derived from the Cole-Cole plot. The resonance phenomenon due to a series L - C - R resonance was usually observed in high frequency range. In order to investigate the trapping phenomena in ZnO grains, Cordaro and Shim presented the relation between the emission rate of electrons and the trapping energy level^[10]. As a result, a common trap energy level of about 0.33 eV is corresponding to the intrinsic defect of ZnO. Furthermore, other trap energy levels would appear depending on the impurities of samples.

In the present work, the influence of Y_2O_3 dopant on microstructure, electrical properties and deep trap levels of ZnO based varistor ceramics has been investigated.

2 Experimental procedure

The samples were prepared by using a classical ceramic sintering procedure. Reagent-grades raw materials were used as a nominal composition of (93.8- x) mol% ZnO, 0.7 mol% Bi_2O_3 , 5.5 mol% ($MnO_2+Cr_2O_3+Co_2O_3 + Sb_2O_3+SiO_2$), and x mol% Y_2O_3 where $x=0, 1, 2$ and 3 (sample labeled as ZY0, ZY1, ZY2 and ZY3, respectively). These raw materials were homogeneously mixed in a planetary mill. The powders were dried at 90°C and pressed under 160 MPa into discs with 20 mm in diameter and 2 mm in thickness. The pellets were sintered at 1200°C for 3 h and cooled down to room temperature in the furnace. Finally, each specimen was polished to about 1.5 mm in thickness, painted with silver slurry in both sides and fired at 600°C for 15 min in air.

The crystalline phase of the samples was analyzed by X-ray powder diffraction (XRD) analysis, which was performed on a Rigaku D/MAX-2550V diffractometer using Cu $K\alpha$ radiation at 40 kV and 100 mA. The microstructures of samples were examined using a scanning electron microscope (SEM). The average ZnO grain sizes of all the samples were determined by the linear intercept method based on their SEM micrographs. The current-voltage (I - V) characteristic of each sample was measured by a DC voltage generator combined with

a multimeter (Model 34401A, Agilent Technologies Inc., USA). The voltages of each varistor sample at 0.1 mA and 1 mA were extracted from the I - V curve to determine its voltage gradient V_N and nonlinear coefficient α . The leakage current of each varistor sample was measured when the applied voltage was $0.75 V_N$.

The dielectric responses of samples were measured over a frequency range from 1 Hz to 20 MHz by the broadband dielectric spectrometer equipped with a cryostat system (Concept 80 Broadband Dielectric Spectrometer, Novocontrol Technologies GmbH & Co. KG, Germany). In order to investigate the temperature dependence of the dielectric behavior and the characteristic of deep trap levels of different varistor samples, the dielectric spectroscopy was acquired in a temperature range from 133 K to 573 K with an interval of 20 K.

3 Results and discussions

The phase composition of ZnO varistors with different Y_2O_3 additions is given in Figure 1, the XRD patterns indicate that ZnO phase, $Zn_7Sb_2O_{12}$ -type spinel phase and γ - Bi_2O_3 phase are observed in the samples without Y_2O_3 . Furthermore, in the samples doped with Y_2O_3 , an additional Y_2O_3 -containing phase is detected and the exact composition of this new phase is difficult to determine. Bernik considered it to be a Bi-Zn-Sb-Y-O phase with traces of oxides of Cr, Mn, Co and Ni by EDS analysis^[5]. With the increasing of Y_2O_3 content, the relative intensity of $Zn_7Sb_2O_{12}$ -type spinel phase decreases, while that of the Y_2O_3 -containing phase

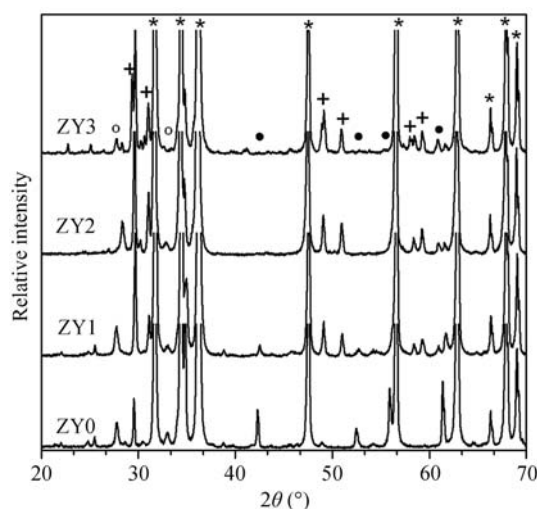


Figure 1 XRD patterns of different ZnO samples doped with different Y_2O_3 additions. *, ZnO phase; +, Y_2O_3 -containing phase; •, $Zn_7Sb_2O_{12}$ -type spinel phase; o, γ - Bi_2O_3 phase.

increases at the same time.

Figure 2 illustrates the SEM micrographs of the ZnO varistor samples, which indicates that the average grain size decreases as the Y_2O_3 addition increases. The average grain sizes of these samples are listed in Table 1. We can observe that the Y_2O_3 -containing phase is grained with a smaller grain size than $Zn_7Sb_2O_{12}$ -type spinels and distributed uniformly along the grain boundary with the introduction of Y_2O_3 . The Y_2O_3 -containing spinels have a similar effect on hindering the grain growth as $Zn_7Sb_2O_{12}$ -type spinels. As a result, the grain growth is markedly suppressed.

The ZnO phase, $Zn_7Sb_2O_{12}$ -type phase and Y_2O_3 -containing phase are identified by EDS analysis and marked with letters and arrows in Figure 2. Moreover, the atom ratios corresponding to the spinel phase are given in Table 2. The $Zn_7Sb_2O_{12}$ -type phase and Y_2O_3 -containing phase coexist in the Y_2O_3 -doped ZnO samples, while only $Zn_7Sb_2O_{12}$ -type phase exists in samples without Y_2O_3 . The Y_2O_3 -containing phase mainly consists of Zn, Sb, Y and O elements with minor

Bi element. However, it is difficult to determine exact chemical composition by EDS due to the small size of these spinel phases and the accuracy of EDS measurement.

The electrical properties of the ZnO varistor samples are summarized in Table 1, as well. It is noticeable that the electrical properties of these samples are greatly influenced by the addition of Y_2O_3 . Owing to the change of grain sizes from about 9.2 μm to 4.5 μm , the voltage gradients of samples increase from 462 V/mm to 2340 V/mm, which means that the voltage gradient of the ZnO varistor can be elevated by increasing Y_2O_3 addition. However, the leakage currents of varistor samples increase from 0.6 μA to 45.4 μA , and their nonlinear coefficients decrease from 22.3 to 11.5. According to previous literatures, the breakdown voltage per grain boundary of different ZnO varistors is about 3 V. Meanwhile, the decrease in average ZnO grain size leads to the increase in the number of grain-grain junction per unit thickness, which means that the breakdown voltage of samples with identical thickness can be improved by

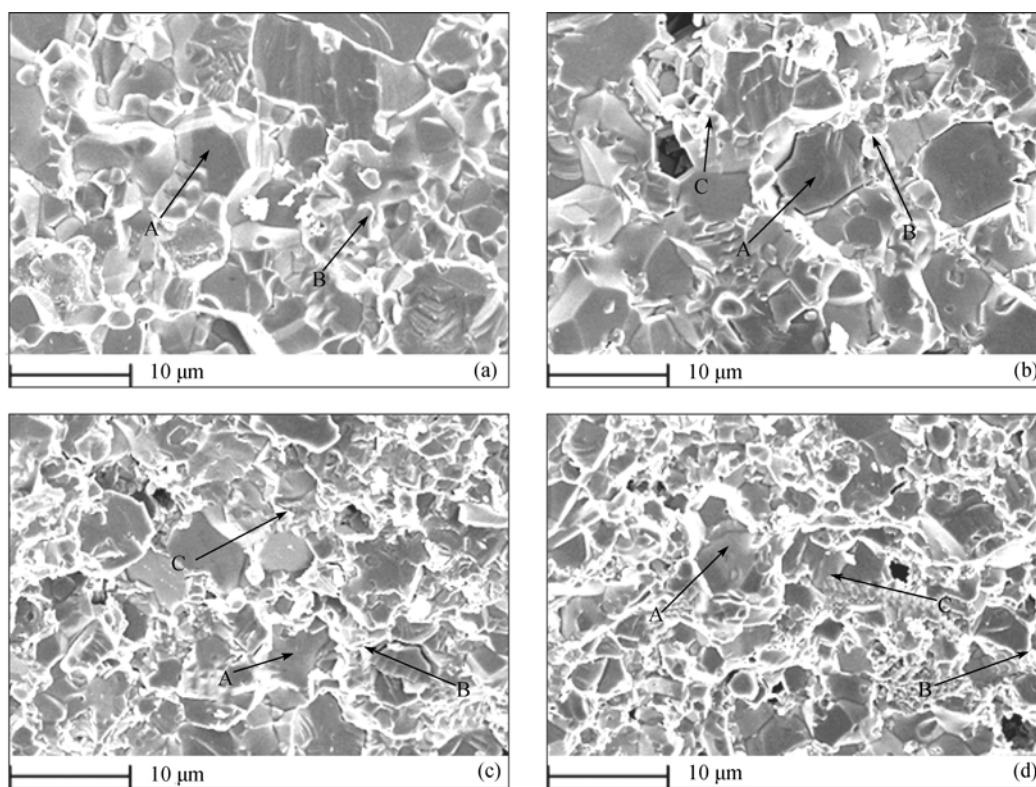


Figure 2 SEM micrographs of the surface structures of the ZnO varistor samples. (a) 0 mol%; (b) 1 mol%; (c) 2 mol%; (d) 3 mol%. A, ZnO phase; B, $Zn_7Sb_2O_{12}$ -type phase; C, Y_2O_3 -containing phase.

Table 1 Grain size and electrical properties of ZnO-based varistor with varied Y₂O₃ addition

Sample	Grain size (μm)	Voltage gradient (V/mm)	Leakage current (μA)	Nonlinear coefficient
ZY0	9.2	462	0.6	22.3
ZY1	7.1	801	3.3	19.2
ZY2	5.6	1078	9.7	16.8
ZY3	4.5	2340	45.4	11.5

Table 2 Atom ratio corresponding to the spinel phase in the investigated samples by EDS analysis

Sample	Spinel type	Zn (%)	Bi (%)	Sb (%)	O (%)	Y (%)
ZY0	B	21.20	0.53	57.94	20.33	–
	C	–	–	–	–	–
ZY1	B	54.24	0.87	24.67	20.22	–
	C	6.34	2.11	68.60	12.85	10.10
ZY2	B	34.03	1.73	54.03	10.21	–
	C	11.91	12.02	61.50	8.97	5.60
ZY3	B	58.27	0.63	13.78	27.32	–
	C	46.04	1.20	27.72	22.68	2.36

hindering the growth of grains. Therefore, the elevation in voltage gradient of these samples should be mostly attributed to the decrease of the grain size. The spinel particles pin ZnO grain boundary and thus control the grain growth. The variation of leakage current and nonlinear coefficient may be related to the formation of Y₂O₃-containing phase which affects the distribution of other dopant cations along the grain boundary. Since the formation of a Bi-Zn-Sb-Y-O phase with trace amount of other added oxides in the Y₂O₃ doped samples, the concentration and distribution of Bi₂O₃ and other additives in the grain boundary will be modified. However, Bi₂O₃ is considered to be an essential additive to improve the nonlinear characteristics. As a result, the leakage current and nonlinear coefficient deteriorate in the samples doped with Y₂O₃.

The dielectric spectroscopies of these ZnO varistor samples at different temperatures are illustrated in Figure 3 in the complex plane. The real and imaginary parts of sample's permittivity decrease as the Y₂O₃ content increases. As shown in Figure 3, it is evident that samples ZY0 and ZY1 have multi relaxation peaks. However, it is hard to extract another relaxation peak from the complex permittivity curves of samples ZY2 and ZY3 which are doped with higher ratios of Y₂O₃. The complex permittivity can be expressed by one conductive term and n relaxation terms as the following equation^[11]:

$$\varepsilon^* = -i \left(\frac{\sigma_0}{\varepsilon_0 \omega} \right)^N + \sum_{k=1}^n \left[\varepsilon_{\infty k} + \frac{\varepsilon_{S_k} - \varepsilon_{\infty k}}{\left(1 + (i\omega_k \tau_k)^{1-\alpha_k} \right)^{\beta_k}} \right], \quad (1)$$

where ε^* is the complex permittivity, the first term of the right side of eq. (1) is the conductive term, n denotes the number of relaxations; τ_k specifies the relaxation time; ω_k is the relaxation angular frequency; ε_{S_k} and $\varepsilon_{\infty k}$ correspond to the static and high-frequency dielectric constants of the k th relaxation term, respectively.

There are three possible cases of relaxation: (a) when $\alpha=0$, $\beta=1$, Debye-like relaxation; (b) when $0<\alpha<1$, $\beta=1$, Cole-Cole-like relaxation; (c) when $0<\alpha<1$, $0<\beta<1$, Havriliak-Negami relaxation^[12]. It is generally considered that the dielectric spectroscopy of a ZnO sample is not a simple Debye case with a single relaxation time but a Cole-Cole type with a distribution of relaxations^[13,14]. The relaxation peak means that a resonance occurs when the emission rate of the electron in a particular energy level equals the angular frequency of the stimulus signal. The characteristic emission rate e_n associated with the trapping level E_t is expressed by^[15]

$$e_n = \tau_n^{-1} = S_n v_{th} N_c \exp[E_t/kT], \quad (2)$$

where S_n is the capture cross-section; v_{th} is the thermal velocity and N_c is the effective density of states for the conduction band.

By measuring the dielectric spectroscopies of the ZnO samples from 133 K to 573 K and fitting the experimental

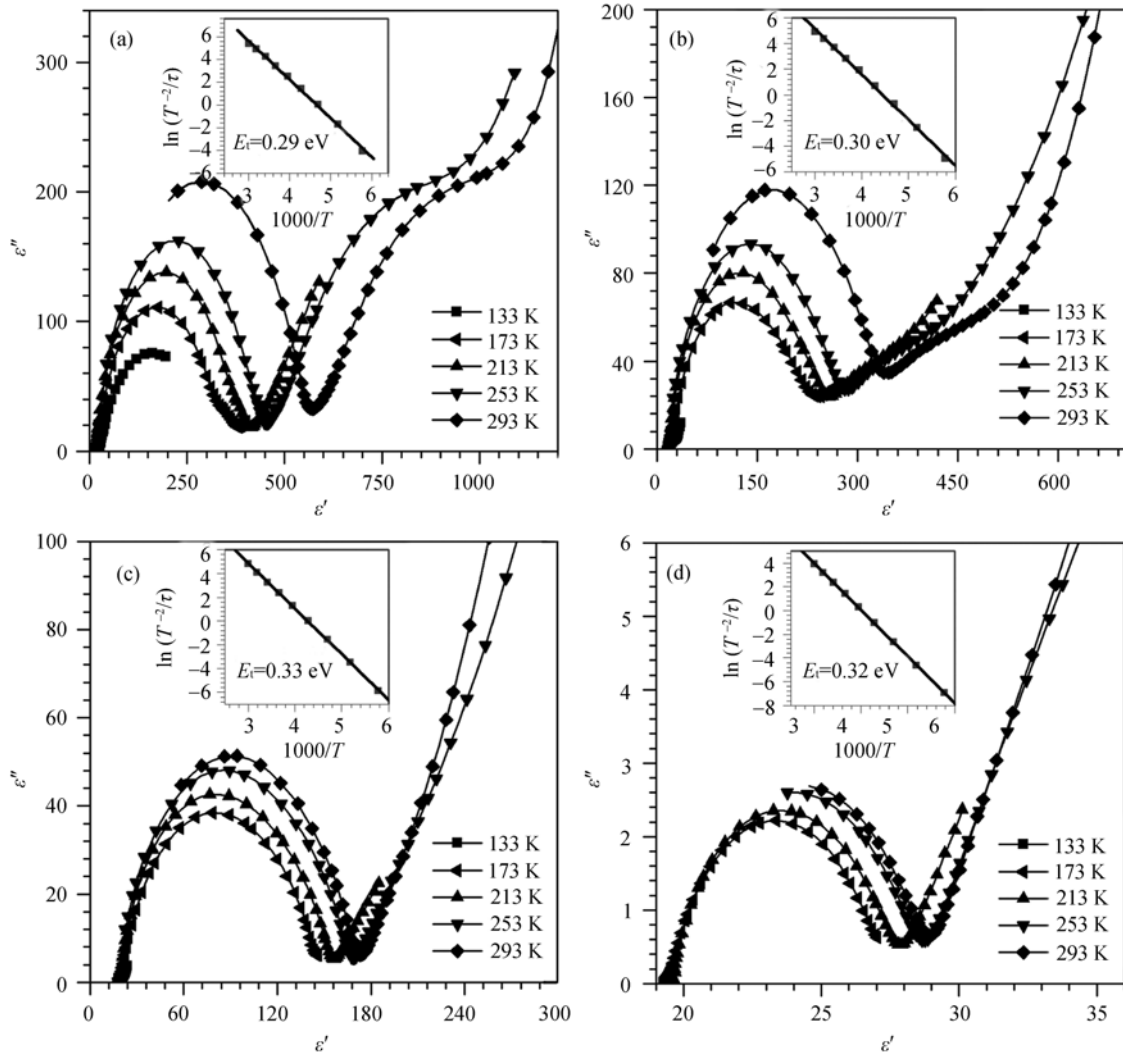


Figure 3 Cole-Cole plot of ZnO varistor samples doped with varied Y_2O_3 in the frequency range from 1 Hz to 20 MHz at different temperatures. (a) 0 mol%; (b) 1 mol%; (c) 2 mol%; (d) 3 mol%.

data according to eq. (1), the plot $\ln(T^{-2}/\tau_n)$ vs $1000/T$ used to demonstrate the temperature dependence of the relaxation time is depicted in the insets of Figures 3(a) to 3(d). The plot can be fitted to a straight line by least-squares fit method, which yields a slope proportional to the trap energy level E_t and an intercept proportional to the capture cross-section S_n as listed in Table 3.

In Table 3, the trap energy and capture cross section generally increase as the ration of Y_2O_3 increases, but the capture cross section of sample ZY3 is slightly less than that of sample ZY2. The results are very close to those in literatures, such as Cordaro and Shim^[10]. The order of the capture cross sections obtained is approximately 10^{-14} cm^2 , which is in the range of an electron trap^[15]. These trap energy levels, of which the small

Table 3 Summary of relaxation time related trapping parameters

Sample	E_t (eV)	S_n (cm^2)
ZY0	0.293 ± 0.005	0.48×10^{-14}
ZY1	0.299 ± 0.006	1.71×10^{-14}
ZY2	0.318 ± 0.004	2.82×10^{-14}
ZY3	0.335 ± 0.002	2.19×10^{-14}

variations are associated with the experimental errors, are around the activation energy of oxygen vacancy V_o^\bullet (about 0.35 eV) in ZnO systems. Furthermore, the characteristics of these traps are independent of the dopants and preparation processes according to the results presented here and in other literatures. Therefore, these traps may originate from the intrinsic defects in ZnO lattice.

4 Conclusions

The introduction of Y_2O_3 causes the formation of an Y_2O_3 -containing phase and the decrease of grain size in ZnO varistors. As a result, it leads to the improvement of their voltage gradients. However, the nonlinear coefficients and leak currents degrade at the same time. The

dielectric spectroscopies reveal that the multiple relaxation peaks are not obvious as the Y_2O_3 ratio increases. The obtained trap energy level and capture cross section vary slightly with the ratio of Y_2O_3 addition. Finally, the results suggest that these traps could be attributed to the intrinsic defects in the ZnO grains.

- 1 Clarke D R. Varistor ceramics. *J Am Ceram Soc*, 1999, 82(3): 485–502
- 2 Gupta T K. Application of zinc oxide varistors. *J Am Ceram Soc*, 1990, 73(7): 1817–1840
- 3 He J L, Hu J, Meng B, et al. Requirement of ultra-high voltage GIS arrester to voltage gradient of metal-oxide varistor. *Sci China Ser E-Tech Sci*, 2009, 52(2): 450–455
- 4 Nan C W, Clarke D R. Effect of variations in grain size and grain boundary barrier heights on the current-voltage characteristics of ZnO varistors. *J Am Ceram Soc*, 1996, 9(12): 3185–3192
- 5 Bernik S, Maček S, Ai B. Microstructural and electrical characteristics of Y_2O_3 -doped ZnO- Bi_2O_3 -based varistor ceramics. *J Eur Ceram Soc*, 2001, 21(10/11): 1875–1878
- 6 Bernik S, Maček S, Ai B. The characteristics of ZnO- Bi_2O_3 -based varistor ceramics doped with Y_2O_3 and varying amounts of Sb_2O_3 . *J Eur Ceram Soc*, 2004, 24(6): 1195–1198
- 7 He J L, Hu J, Lin Y H. ZnO varistors with high voltage gradient and low leakage current by doping rare-earth oxide. *Sci China Ser E-Tech Sci*, 2008, 51(6): 693–701
- 8 Alim M A. Complex plane analysis of trapping phenomena in zinc oxide based varistor grain boundaries. *J Appl Phys*, 1998, 63(7): 2337–2345
- 9 Alim M A, Li S T, Liu F Y, et al. Electrical barriers in the ZnO varistor grain boundaries. *Phys Stat Sol (a)*, 2006, 203(2): 410–427
- 10 Cordaro J F, Shim Y. Bulk electron traps in zinc oxide varistors. *J Appl Phys*, 1986, 60(12): 4186–4190
- 11 Havriliak S, Negami S. A complex plane representation of dielectric and mechanical relaxation processes in some polymers. *Polymer*, 1967, 8: 161–210
- 12 Bueno P R, Varela J A, Longo E. Admittance and dielectric spectroscopy of polycrystalline semiconductors. *J Eur Ceram Soc*, 2007, 27(13/15): 4313–4320
- 13 Daniel V V. Empirical methods for the evaluation of dielectric measurements. *Dielectric Relaxation*. London: Academic Press, 1967. 95–109
- 14 Abdullah K A, Bui A, Loubiere A. Low frequency and low temperature behavior of ZnO-based varistor by ac impedance measurements. *J Appl Phys*, 1991, 69(7): 4046–4052
- 15 Blatter G, Greuter F. Carrier transport through grain boundaries in semiconductors. *Phys Rev B*, 1986, 33(6): 3952–3966